J. Biochem. **135**, 53–64 (2004)
DOI: 10.1093/jb/mvh006

Properties of Two Distinct Heme Centers of Cytochrome b_{561} from Bovine Chromaffin Vesicles Studied by EPR, Resonance Raman, and Ascorbate Reduction Assay

Fusako Takeuchi[1,2], Hiroshi Hori[3], Eiji Obayashi[*,4], Yoshitsugu Shiro[4] and Motonari Tsubaki[†,1,2,5]

[1]Department of Life Science, Graduate School of Science, Himeji Institute of Technology, Kamigoori-cho, Akou-gun, Hyogo 678-1297; [2]Department of Molecular Science and Material Engineering, Graduate School of Science and Technology, Kobe University, Rokkodai-cho, Nada-ku, Kobe, Hyogo 657-8501; [3]Division of Biophysical Engineering, Department of Systems and Human Science, Graduate School of Engineering Science, Osaka University, Machikaneyama-cho, Toyonaka, Osaka 560-8531; [4]Biophysical Chemistry Laboratory, RIKEN, Harima Institute, Mikazuki-cho, Sayo-gun, Hyogo 679-5148; and [5]CREST, JST.

Received June 2, 2003; accepted November 6, 2003

Cytochrome b_{561} from bovine adrenal chromaffin vesicles contains two hemes *b* with different midpoint potentials (+150 and +60 mV) and participates in transmembrane electron transport from extravesicular ascorbate to an intravesicular monooxygenase, dopamine β-hydroxylase. Treatment of oxidized cytochrome b_{561} with diethylpyrocarbonate caused a downshift of midpoint potential for the lower component, and this shift was prevented by the presence of ascorbate during the treatment. Present EPR analyses showed that, upon the treatment, the g_z = 3.69 heme species was converted to a non-ascorbate-reducible form, although its g_z-value showed no appreciable change. The treatment had no effect on the other heme (the g_z = 3.13 species). Raman data indicated that the two heme *b* centers adopt a six-coordinated low-spin state, in both the reduced and oxidized forms. There was no significant effect of diethylpyrocarbonate-treatment on the Raman spectra of either form, but the reducibility by ascorbate differed significantly between the two hemes upon the treatment. The addition of ferrocyanide enhanced both the reduction rate and final reduction level of the diethylpyrocarbonate-treated cytochrome b_{561} when ascorbate was used as a reductant. This observation suggests that ferrocyanide scavenges monodehydroascorbate radicals produced by the univalent oxidation of ascorbate and, thereby, increases both the reduction rate and the final reduction level of the heme center on the intravesicular side of the diethylpyrocarbonate-treated cytochrome. These results further clarify the physiological role of this heme center as the electron donor to the monodehydroascorbate radical.

Key words: ascorbate, cytochrome b_{561}, EPR, heme redox potential, resonance Raman, transmembrane electron transfer.

Abbreviations: AsA, ascorbate; MDA, monodehydroascorbate; DEPC, diethylpyrocarbonate; MALDI-TOF, matrix-assisted laser desorption/ionization-time of flight.

Brain and neuroendocrine tissues have the highest ascorbate (AsA[3]) levels of any organ system (*1*) because of the presence of a specific AsA transporter system into neuron cells (*2*) that maintains the steep intra/extracellular concentration gradient. In neurosecretory vesicles, such as adrenomedullary chromaffin vesicles and pituitary neuropeptide secretory vesicles, intravesicular AsA (about 20 mM) functions as the electron donor for copper-containing monooxygenases including dopamine β-hydroxylase and peptidyl-glycine α-amidating monooxygenase (*3*, *4*). Upon these monooxygenase reactions, the monodehydroascorbate (MDA) radical is produced within the vesicles by the univalent oxidation of AsA (*5*). Neither AsA nor the MDA radical can pass through vesicle membranes, although dehydroascorbate, the fully-oxidized neutral form, can pass through membranes *via* diffusion (*6–8*). Midpoint potentials for AsA/MDA radicals and for MDA radical/dehydroascorbate are +330 mV and –210 mV, respectively (*9*). It is believed that the intravesicular MDA radical is reduced back to AsA by membrane-spanning cytochrome b_{561}, and, subsequently, the oxidized cytochrome b_{561} is reduced by AsA on the extravesicular side (about 5 mM). Thus cytochrome b_{561} acts as a neuroendocrine-specific transmembrane electron transporter. Indeed, among various cytochromes, cytochrome b_{561} is unique in its localization to neuroendocrine cells in the adrenal medulla, pituitary and different regions of the brain (*10*, *11*) and peripheral nervous system (*12*).

Cytochrome b_{561} is a highly hydrophobic hemoprotein (*13*, *14*) with a molecular mass of 29 kDa (*14*, *15*). We

[*]Present address: MRC Laboratory of Molecular Biology, Structural Division, Hills Road, Cambridge CB2 2QH, UK.
[†]To whom corresponding should be addressed. Tel/Fax: +81-78-803-6582, E-mail: mtsubaki@kobe-u.ac.jp

found that purified cytochrome b_{561} contains two distinct heme *b* centers, with one heme *b* showing a usual low spin EPR signal (g_z = 3.14) and the other giving a highly anisotropic low spin EPR signal (g_z = 3.70) (*16*), as observed in chromaffin vesicle membranes (*17*). Based on a comparison of the deduced amino acid sequences of cytochrome b_{561} from various animals (*18–21*), we have proposed a structural model of cytochrome b_{561} (*22*) by extending the model of Degli Esposti (*23*). In our model, there are two fully conserved regions in the sequences, the first (^{69}ALLVYRVFR^{77}) located on the extravesicular side of an α-helical segment, and the second (^{120}SLHSW^{124}) in an intravesicular loop connecting two α-helical segments (*22*). Accordingly, we proposed that the two hemes *b* were likely to be located on opposite sides of the vesicular membrane in close contact with these putative binding sites (for the extravesicular AsA and intravesicular MDA radical, respectively) (*22*).

Our pulse radiolysis analysis of cytochrome b_{561} indicated that the two heme *b* centers have distinct roles in electron donation to the MDA radical and electron acceptance from AsA, respectively (*24*). We found that the electron accepting ability from AsA is selectively destroyed by treating oxidized cytochrome b_{561} with diethylpyrocarbonate (DEPC) (*25*). However, the electron donating activity from the reduced heme *b* center to the MDA radical was retained after the treatment (*25*). We found that two fully conserved histidyl residues (His88 and His161), possible heme ligands on the extravesicular side, and one well-conserved lysyl residue (Lys85) are selectively *N*-carbethoxylated upon DEPC treatment (*25*). The electron accepting ability from AsA, however, could be protected by the presence of AsA during the DEPC treatment, suggesting that the AsA-binding site is on the extravesicular side (*26*, *27*). We observed that the purified cytochrome b_{561} shows a sigmoidal shape upon redox titration, consistent with the presence of two heme *b* redox centers with slightly different midpoint potentials (+170 and +60 mV) (*28*), and that the treatment of oxidized cytochrome b_{561} with DEPC causes a downshift of the midpoint potential for the lower redox component (*26*). All these pieces of evidence seem to favor our 6 trans-membrane helices model containing two heme *b* centers (*22*) and to be incompatible with the 5 transmembrane helices model with a single heme *b* center (*19*).

Kamensky *et al*., however, reported recently that cytochrome b_{561} has an additional low spin heme center in chromaffin vesicle membranes based on EPR and circular dichroism spectra (*29*). They proposed that cytochrome b_{561} forms a dimer, with one heme *b* per monomer and one heme *b* residing between the interface s of two monomers (*30*). Other group proposed that, based on alkaline denaturation experiments of oxidized cytochrome b_{561}, the heterogeneity of the heme center could occur due to pH-induced alteration and oxidative destruction and can explain the complicated nature of cytochrome b_{561} (*31*). They, therefore, raised some serious questions regarding the two-heme-model of cytochrome b_{561} (*31*). On the other hand, a new member of cytochrome b_{561} family was identified in plasma membranes of duodenal enterocytes (*32*, *33*). Dcytb (for duodenal cytochrome b_{561}) was reported to be responsible for physiological ferric reductase activity in the duodenal mucosa and an important element in the iron absorption pathway (*32*). Cytochrome b_{561} and Dcytb share a similar membrane topology and potential histidyl heme ligands, indicating that Dcytb might bind two hemes too. Putative binding sites for AsA and the MDA radical are also conserved in Dcytb, suggesting that Dcytb may react with one or more of these compounds (*32*). Other members of the cytochrome b_{561} family are also known to be present in various plasma membranes such as rabbit neutrophils (*34*) and plant cells (*35*, *36*). More distant members of the cytochrome b_{561} family are now emerging (*37*).

Thus, elucidation of precise structures of the heme redox centers of cytochrome b_{561} is increasingly important and will be very valuable to clarify the physiological roles of these new members of the transmembrane electron carrier. In the present study, we conducted EPR and resonance Raman spectroscopic analyses together with an AsA-reduction assay on the purified cytochrome b_{561} to clarify the structure of the heme moieties and the effect of the DEPC-modification.

MATERIALS AND METHODS

Purification of Cytochrome b_{561}—Cytochrome b_{561} was purified as described previously (*16*). The purity of cytochrome b_{561} was determined from its visible absorption spectrum, heme content analysis, and SDS-polyacrylamide gel electrophoresis (*16*). The concentration of cytochrome b_{561} was determined using a millimolar extinction coefficient of 267.9 mM^{-1} cm^{-1} at 427 nm in the reduced form (*16*).

Modification of Cytochrome b_{561} with Diethylpyrocarbonate—The concentrated cytochrome b_{561} solution was acidified to pH 6.5 by adding 0.5 M potassium-phosphate buffer (pH 6.0) and oxidized by the step-wise additions of potassium ferricyanide solution (100 mM). Complete oxidation was confirmed by visible absorption spectroscopy. The oxidized cytochrome b_{561} was gel-filtered through a PD-10 column (Amersham Pharmacia Biotech) equilibrated with 50 mM potassium-phosphate buffer (pH 6.0) containing 1.0% (w/v) octyl β-glucoside, and then diluted with the same buffer to an appropriate concentration. The diluted sample in the oxidized form was treated with various concentrations of DEPC for 30 min, as previously described (*25*). The DEPC treatment of cytochrome b_{561} in the presence of 20 mM of sodium ascorbate was done similarly. The DEPC-treated samples (either in the oxidized form or in the presence of 20 mM AsA) were then gel-filtered through a PD-10 column equilibrated with 50 mM potassium-phosphate buffer (pH 6.0) containing 1.0% (w/v) octyl β-glucoside to remove DEPC (and AsA, if any). A part of the DEPC-treated cytochrome b_{561} sample was then analyzed for reactivity with AsA and the integrity of the heme moiety at 20°C using a Shimadzu UV-2400PC spectrophotometer (Kyoto).

Redox Titrations—Spectrophotometric redox titrations were performed essentially as described by Dutton (*38*) with several modifications as described previously (*26*) using a UV-2400PC spectrometer equipped with a thermostatted cell holder connected to a thermobath (RC6 CS, LAUDA,). Electrode potentials are expressed relative to a standard hydrogen electrode.

Measurements of EPR Spectra—The oxidized cytochrome b_{561} samples (either control, DEPC-treated in the oxidized form, or DEPC-treated in the presence of 20 mM AsA) in 50 mM sodium-phosphate buffer (pH 6.5) containing 1.0% (w/v) octyl β-glucoside were concentrated to about 230 μM with a 50-ml Amicon concentrator fitted with a membrane filter (Millipore PTTK04310; pore size 30,000 NMWL). The concentrated samples were introduced into EPR tubes and frozen in liquid nitrogen (77K). To obtain AsA-reduced forms, a small volume of concentrated AsA solution was added aerobically to the oxidized forms of cytochrome b_{561} (final AsA concentration, 20 mM). The samples were then left at room temperature for 30 min to insure complete equilibrium, transferred to EPR tubes, and then frozen in liquid nitrogen. EPR measurements were carried out at X-band (9.23 GHz) microwave frequency with a Varian E-12 EPR spectrometer with 100-kHz field modulation. An Oxford flow cryostat (ESR-900) (from 5 to 20K) was used. The microwave frequency was calibrated with a microwave frequency counter (Takeda Riken, Model TR5212). The strength of the magnetic field was determined with an NMR field meter (ECHO Electronics, Model EFM 2000AX). The accuracy of the g-values was approximately ±0.001.

Measurements of Resonance Raman Spectra—The purified cytochrome b_{561} (13–18 μM) in 50 mM potassium-phosphate buffer (pH 6.0) containing 1.0% (w/v) octyl β-glucoside was placed in an air-tight Raman cell. Resonance Raman scattering was obtained with the 441.6-nm line of a He/Cd laser (Kimmon Electrics, Model IK5651R-G), and with the 413.1- and 406.7-nm lines of a Kr^+ ion laser (Coherent, Model Innova 90C). The scattering light (90°) was detected with a CCD detector (100K) attached to a 1-m single monochromator (JASCO NR-1800). Holographic filters (KAISER OPTICAL SYSTEMS, Inc.) were used to remove the Raleigh scattering. The slit-width and slit-height were set to 90 μm and 10 mm, respectively. The excitation laser beam was focused on the sample to be about 50 μm in diameter, and the laser power (at the sample point) was adjusted to 50 mW. Accumulation times were 900 s (60 s × 15) for all measurements. All measurements were carried out at room temperature (~20°C) with the Raman cell spun at 3500 rpm. Raman shifts were calibrated with indene and the accuracy of the peak positions of the Raman bands was ±1 cm^{-1}. A small volume of concentrated AsA solution was added aerobically to reduce the oxidized cytochrome b_{561} (final AsA concentration, 2 mM). The sample solution was then left at room temperature for 30 min to insure complete equilibrium, and transferred to a Raman cell. For the full reduction of the cytochrome, a small volume of N_2-saturated dithionite solution was added anaerobically to the sample solution in the Raman cell to a final concentration of 10 mM.

Effects of Ferricyanide/Ferrocyanide on the Reduction of the DEPC-Treated Cytochrome b_{561} with AsA—Effects of the additions of ferricyanide (final; 0.01, 0.05, 0.1 mM), ferrocyanide (final; 0.01, 0.05, and 0.1 mM), and Fe^{3+}-EDTA (final; 0.1, 2.0 mM) on the reduction rate and final reduction level of cytochrome b_{561} (1.5 μM) (either for the DEPC-treated or control samples) in 50 mM potassium-phosphate buffer (pH 6.0) containing 1.0% (w/v) octyl β-glucoside using AsA (2.0 mM) as a reductant were examined. Changes in absorbance at 561 nm at 20°C were recorded with a UV-2400PC spectrophotometer.

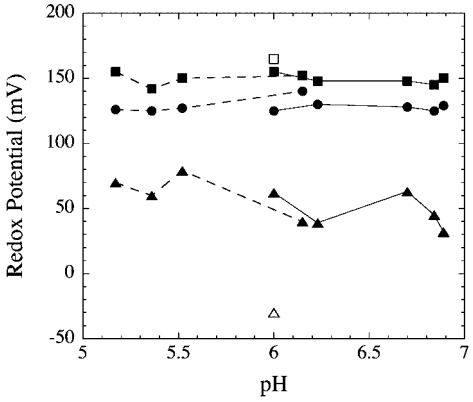

Fig. 1. **The pH-dependency of redox behaviors of cytochrome b_{561}.** The concentration of cytochrome b_{561} was 10 μM in either 50 mM potassium-phosphate buffer or 50 mM sodium acetate buffer containing 1.0% (w/v) octyl β-glucoside and various redox mediators (details are described in Ref. *26*). Solid circles indicate the apparent midpoint potentials; solid squares and triangles indicate the upper and lower midpoint potentials, respectively. Solid lines represent the measurements in potassium phosphate buffer (pH 6.00, 6.23, 6.70, and 6.89); broken lines represent the measurements in sodium acetate buffer (pH 5.17, 5.36, 5.52, and 6.15). For comparison, upper and lower midpoint potentials of DEPC-treated cytochrome b_{561} (in the oxidized form) are shown as the open square and open triangle (measured at pH 6.0) (*26*), respectively.

RESULTS

Midpoint Redox Potential—The potentiometric behavior of purified cytochrome b_{561} measured at various pH (from 5.17 to 6.89) showed good agreement between points obtained during reductive and oxidative titrations. The apparent midpoint potentials were estimated to be around +125 mV, regardless of the medium pH (Fig. 1; solid circles), consistent with a previous observation of Apps *et al*. (*39*) using membrane preparations. Nernst plot [*i.e.*, redox potential *vs.* $\log_{10}([ox]/[red])$] analyses of the data showed the upper and lower asymptotic potentials to be around +150 and +60 mV, respectively (Fig. 1; solid squares and solid triangles), consistent with our previous report (*26*), and did not show any appreciable pH-dependence in the region from 5.15 to 6.89 (Fig. 1). At alkaline pH, oxidized cytochrome b_{561} became very unstable as previously reported (*22*). Even at pH 7.0, a significant part of the oxidized form became non-reducible during longer storage on ice. Therefore, the redox titrations that require several hours for completion were not conducted above pH 7.0 in the present study.

Treatment of cytochrome b_{561} in the oxidized form with DEPC (0.5 mM) caused a drastic change in redox behavior. One heme *b* component with a lower midpoint potential showed a significant lowering of the asymptotic potential to as low as –30 mV (Fig. 1; open triangle), as reported previously (*26*). On the other hand, the higher asymptotic potential did not show any appreciable change upon the treatment (Fig. 1; open square) (*26*). The presence of 20 mM AsA during DEPC treatment inhibited the downshift of the lower asymptotic potential

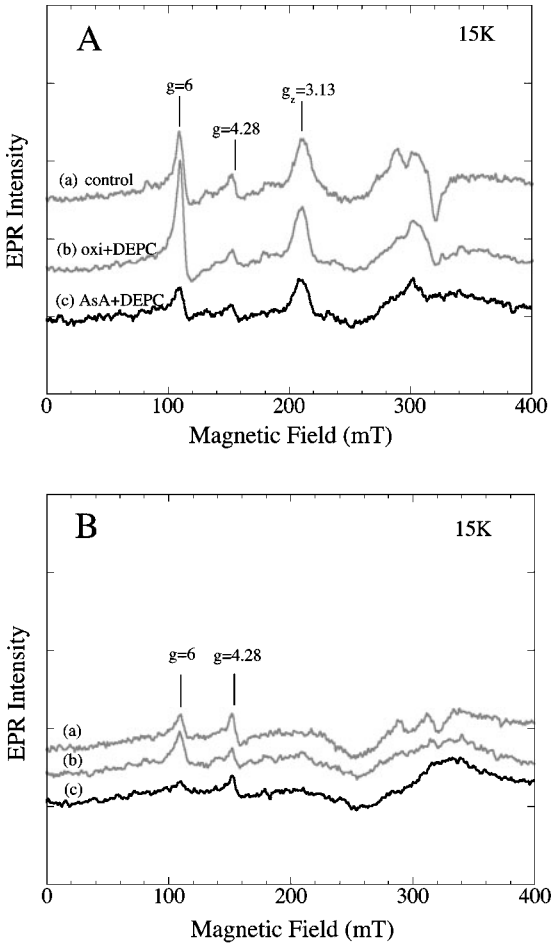

Fig. 2. **X-band EPR spectra of cytochrome b_{561} measured at 15K.** Panel A shows spectra in the oxidized form; panel B shows spectra in the AsA-reduced form. For panel B, the final concentration of AsA was 20 mM. In each panel, control (trace a), DEPC-treated in the oxidized form (trace b), and DEPC-treated in the presence of AsA (20 mM) (trace c) cytochrome b_{561} are shown.

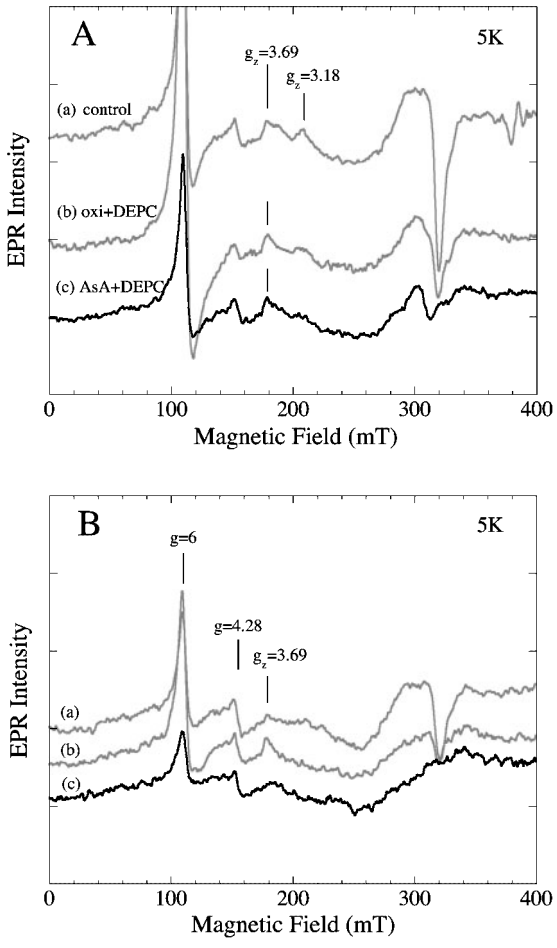

Fig. 3. **X-band EPR spectra of cytochrome b_{561} measured at 5K.** Panel A shows spectra in the oxidized form, whereas panel B shows spectra in the AsA-reduced form. Other conditions are the same as in Fig. 2.

almost completely (*26*). Thus, the protective effect of AsA against the peculiar redox behavior caused by the DEPC-modification was significant, as previously reported (*26*).

EPR Spectroscopy—At 15K, the EPR spectrum of the oxidized cytochrome b_{561} showed a clear low-spin signal at g_z = 3.13, in addition to the signals from a small amount of high-spin species (at g = 6) and the adventitious iron at g = 4.28 [Fig. 2A (a)], as previously reported (*16*). The g_z = 3.13 signal did not show any appreciable change upon treatment with DEPC (0.5 mM) either in the oxidized form or in the presence of 20 mM AsA [Fig. 2A (b, c)]. Reduction of these DEPC-treated samples with AsA (20 mM) caused an almost complete loss of the g_z = 3.13 signal [Fig. 2B (b, c)], as observed for the control sample [Fig. 2B (a)]. This observation suggests that the low-spin species with the g_z = 3.13 signal does not suffer from DEPC-modification and is fully reducible by AsA.

There were two low-spin signals in the EPR spectrum of oxidized cytochrome b_{561} measured at 5K [Fig. 3A (a)]. The g_z = 3.18 signal corresponding to the g_z = 3.13 signal observed at 15K was much weaker in intensity than the other low-spin signal at g_z = 3.69. This highly anisotropic low-spin signal at g_z = 3.69 did appear only at extreme low temperatures below 10K, as previously reported (*16*). The present results showed that the g_z = 3.69 signal did not disappear after oxidation/gel-filtration, in complete contrast with the observations of Wanduragala *et al*. (*31*) and, therefore, indicate that the g_z = 3.69 species is an intrinsic heme component of cytochrome b_{561}. It must be noted that the relative intensities of the g_z = 3.13 and the g_z = 3.69 signals seem to be very dependent on the nature of the protein environment. This was verified by the observation of two strong EPR signals at g_z = 3.13 and g_z = 3.69 with similar intensities at 11K or 15K in chromaffin vesicle membranes (*17*, *29*). The membraneous environment in chromaffin vesicles may cause a significant difference in the spin-lattice relaxation time, particularly for the g_z = 3.69 species, from those in the detergent-solubilized state, leading to a considerable difference in the temperature dependency of the EPR spectra (*16*, *17*, *29*).

Treatment of cytochrome b_{561} with DEPC (0.5 mM) either in the oxidized form or in the presence of AsA (20 mM) caused no appreciable change in the g_z = 3.69 signal at 5K for the oxidized form [Fig. 3A (b, c)]. The g_z = 3.69 signal of the sample treated with DEPC in the oxidized form retained its full intensity even after a longer period

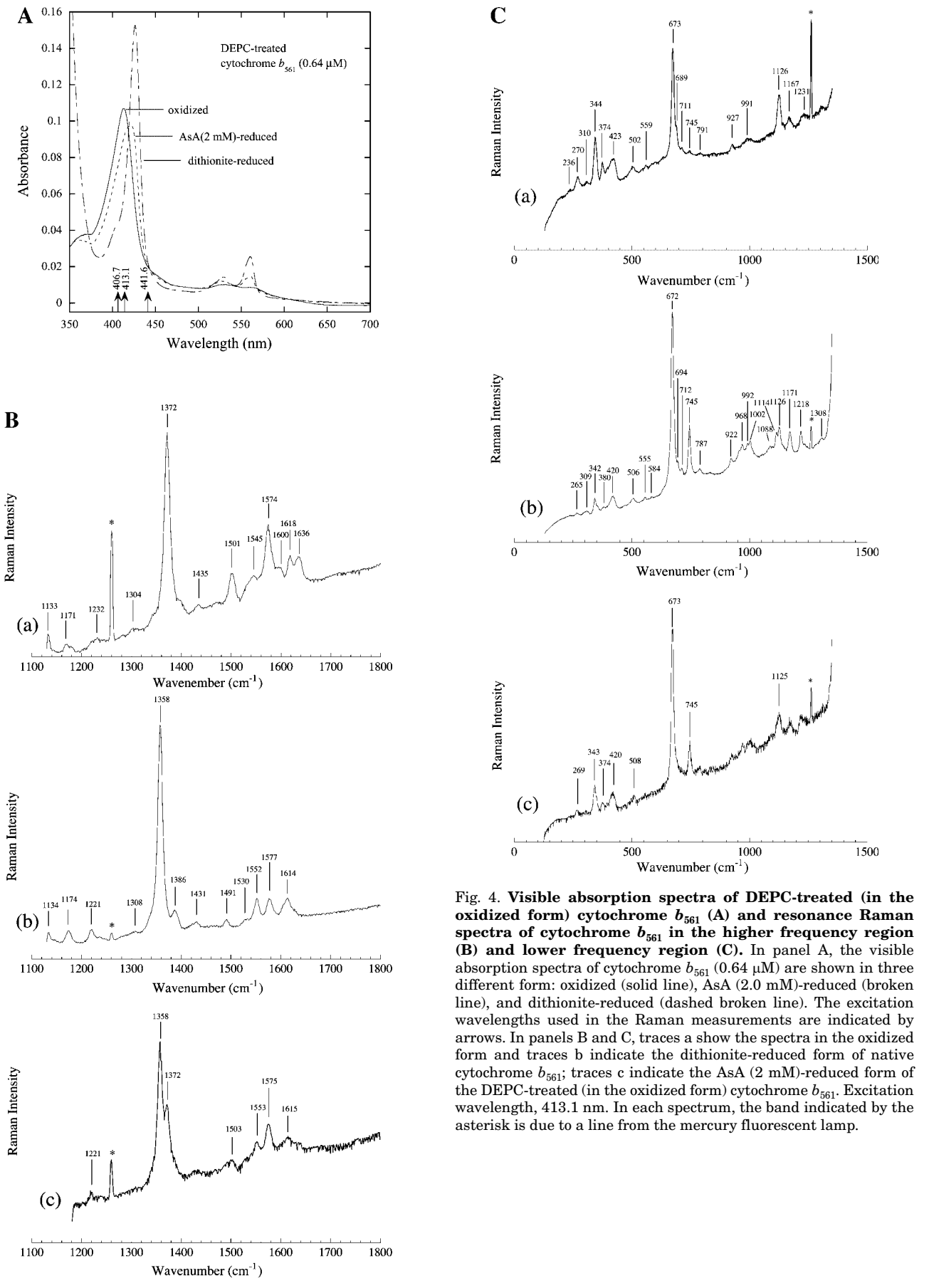

Fig. 4. **Visible absorption spectra of DEPC-treated (in the oxidized form) cytochrome b_{561} (A) and resonance Raman spectra of cytochrome b_{561} in the higher frequency region (B) and lower frequency region (C).** In panel A, the visible absorption spectra of cytochrome b_{561} (0.64 μM) are shown in three different form: oxidized (solid line), AsA (2.0 mM)-reduced (broken line), and dithionite-reduced (dashed broken line). The excitation wavelengths used in the Raman measurements are indicated by arrows. In panels B and C, traces a show the spectra in the oxidized form and traces b indicate the dithionite-reduced form of native cytochrome b_{561}; traces c indicate the AsA (2 mM)-reduced form of the DEPC-treated (in the oxidized form) cytochrome b_{561}. Excitation wavelength, 413.1 nm. In each spectrum, the band indicated by the asterisk is due to a line from the mercury fluorescent lamp.

Table 1. **Resonance Raman spectral bands and their assignments to cytochrome b_{561} in comparison with heme model complexes.**

Mode	$[(Im)_2Fe^{3+}]^+$		cyt b_{561} (ox)	$(Im)_2Fe^{2+}$		cyt b_{561}(red)
	PP	ΔMP		PP	ΔMP	
Skeletal modes						
ν_{10}	1,640		1,636	1,617		1,614
ν_{37}	1,602		1,600	1,604		
ν_2	1,579	+13	1,574	1,584	+15	1,577
ν_{38}	1,554		1,545	1,560		1,552
ν_3	1,502		1,501	1,493		1,491
ν_{28}	(1,469)			(1,461)		
ν_{20}	(1,399sh)			(1,392sh)	+2	1,386
ν_4	1,373		1,372	1,359		1,358
$\nu_6+\nu_8$	1,130		1,126	1,130		1,126
$\nu_{32}+\nu_{35}$	(972)	+9		(972)	+1	968
ν_6	(804)	+1		(819)	13	
ν_{16}	749	0	745	748	4	745
ν_7	677	0	673	675	0	672
ν_{49}	(561)	–	(559)	(558)	–	(555)
pyr fold	(510)	+15	502	(507)	–	506
pyr fold	(425)	30		(426)	–	420
$2\nu_{35}$	(380)	1	374	–	–	
ν_9	(276)	11	270	(263)	2	(265)
Peripheral modes						
ν (C=C)	1,620		1,618	1,620		1,614
$\delta_s(=CH_2)$	1,435		1,435	(1,431)		1,431
ν_{21}	(1,306)	–	(1,304)	(1,305)	–	(1,308)
ν_{13}	1,230	–	1,232	1,225	+3	1,218
ν $(C_b\text{-}C_\alpha)^{(1)}$	1,167		1,171	1,174		1,171
$\delta_{as}(=CH_2)$	(1,089)			(1,089)		(1,088)
γ(CH=)	(1,008)			(1,008)		1,002
ν_{45}	997	+4	(991)	995	+1	(992)
ν_{46}	(951)	0		(925)	+14	922
ν_{32}	(791)	–	791	(791)	–	787
ν_{47}	(714)	2	711	(717)	–	712
$\delta(C_bC_\alpha C_\beta)^{(1)}$	(419)		423	(412)		420
$\gamma(C_bS)$		–	374	(384)	–	(380)
ν_8	349	0	344	345	0	342
$\delta(C_bC_\alpha C_\beta)^{(2)}$	(312)			(312)		
$\gamma(C_mC_a)$	296	6		298	+8	
ν (Fe-Im)	(199)			(201)		

Excitation wavelength, 413.1 nm; numbers in parentheses indicate very weak bands. Mode numbers and skeletal assignments follow Abe *et al*. (*62*). Frequencies for the $[(Im)_2Fe^{3+}PP]^+$, $(Im)_2Fe^{2+}PP$, $[(Im)_2Fe^{3+}MP]^+$ and $(Im)_2Fe^{2+}MP$ complexes were taken from Choi and Spiro (*41*, *42*). PP and MP denote protoporphyrin IX and mesoporphyrin IX, respectively. ΔMP indicates the frequency downshifts observed on substituting MP for PP; up shifts are indicated by +. The – marks in the ΔMP columns indicate the absence of a description in the original references. The sh mark indicates a shoulder band.

of incubation with 20 mM of AsA [Fig. 3B (b)]. The addition of a stronger reductant, sodium dithionite, however, caused a complete disappearance of the g_z = 3.69 signal (spectra not shown). These observations indicate that the heme *b* center producing the g_z = 3.69 signal became non-reducible with AsA (but fully reducible with sodium dithionite) upon treatment with DEPC in the oxidized form. On the other hand, the presence of AsA during the DEPC treatment protected the g_z = 3.69 species against conversion to the non-AsA-reducible form and, therefore, the g_z = 3.69 signal disappeared upon the addition of AsA as shown in Fig. 3B (c).

Resonance Raman Spectroscopy—The resonance Raman spectra of cytochrome b_{561} are reported here for the first time. Representative spectra in the higher frequency region (Fig. 4B) of the oxidized (trace a) and dithionite-reduced (trace b) forms excited at 413.1 nm are shown. The spectra of the AsA-reduced form (not shown) were almost identical to those of the dithionite-reduced form, consistent with the notion that 2 mM of AsA can reduce the heme center by as much as ~85% based on the visible absorption spectra (*25*). The most prominent ν_4 bands at 1,372 cm^{-1} for the oxidized (trace a) and 1,358 cm^{-1} for the dithionite-reduced form (trace b), which are explained as reflecting π-delocalization (*40*), are consistent with the fully-oxidized and fully-reduced heme centers, respectively. Other distinct Raman bands of the oxidized form in the higher frequency region, including ν_{10} = 1,636 cm^{-1}, ν_2 = 1,574 cm^{-1}, and ν_3 = 1,501 cm^{-1} (trace a), indicate that both of the two heme centers adopt a six-coordinated

low-spin state (Table 1), consistent with the previous and present EPR studies. Corresponding Raman bands of the dithionite-reduced form at ν_{10} = 1,614 cm^{-1}, ν_2 = 1,577 cm^{-1}, and ν_3 = 1,491 cm^{-1} (trace b) suggest that both of the reduced heme centers also adopt a six-coordinated low-spin state (Table 1). In the lower frequency region excited at 413.1 nm, there were strong ν_7 bands at 673 cm^{-1} in the oxidized (trace a) and at 672 cm^{-1} in the reduced (trace b) forms (Fig. 4C). Other Raman bands, including ν_{16} = 745 cm^{-1}, ν_{49} = 559 cm^{-1}, and ν_9 = 270 cm^{-1}, were assignable to the porphyrin skeletal modes (Fig. 4C; Table 1).

Peripheral vinyl modes of heme *b* (*41*) assignable to $\nu_{(C=C)}$ = 1,618 cm^{-1}, $\delta_{s(=CH2)}$ = 1,435 cm^{-1}, and $\nu_{(Cb\text{-}C\alpha)}$ = 1,171 cm^{-1} were observed in the oxidized spectrum (Fig. 4B, trace a) (Table 1). In the reduced form (trace b), corresponding modes were observed at 1,614, 1,431, and 1,171 cm^{-1}, respectively (Table 1). In the lower frequency region, two bands at 419 and 312 cm^{-1} of the $[(Im)_2Fe^{3+}PP]^+$ complex were assigned to in- and out-of-phase bending of the vinyl groups, $\delta(C_bC\alpha C\beta)$ (*42*). The higher of these two modes was observed for both the oxidized and reduced forms (traces a and b) (Table 1). The presence of these Raman bands attributable to motions of heme vinyl substituent groups is consistent with the macrocycle being protoporphyrin IX, an assignment made previously based on the optical absorption spectra (*16*, *43*). The frequencies of the Raman bands are also very similar to those previously reported for cytochrome b_{558} in the NADPH oxidase of neutrophils (*44*, *45*), and to some extent to chloroplast cytochrome b_{559} (*46*) and cytochrome b_5 (*47*, *48*). It must be noted, however, that there was nothing to indicate a structural difference between the two heme *b* centers in the native cytochrome.

The resonance Raman spectra upon excitation at 406.7 and 441.6 nm were also measured for the oxidized, AsA-reduced, and dithionite-reduced forms. The spectra upon excitation at 406.7 nm were very similar to those obtained at 413.1-nm excitation (spectra not shown). Upon excitation with a 441.6-nm line, the spectra were quite feature-less (except for the ν_2, ν_3, ν_4, ν_7, and ν_{16} bands) due to the off-resonance with the excitation wavelength from the Soret band (spectra not shown) (Fig. 4A).

The effect of DEPC-treatment on the Raman spectra was then examined in both higher and lower frequency regions. For the oxidized form, there was no difference in the Raman spectra between control and DEPC-treated (in the oxidized form) cytochrome b_{561} (spectra not shown). Also, there was no difference for the dithionite-reduced cytochrome b_{561} (spectra not shown). For the AsA-reduced form, there was a clear difference in both the higher (Fig. 4B, trace c) and lower (Fig. 4C, trace c) frequency regions. In both regions, the spectra of the AsA-reduced form of the DEPC-treated sample had the appearance of a mixture of the oxidized and the dithionite-reduced forms. This is apparently due to the partial reduction of the heme *b* centers caused by the loss of electron accepting ability from AsA, as indicated in the visible absorption spectrum (Fig. 4A). It might be expected that the subtraction of the fully reduced spectrum from the partially-reduced spectrum would produce the spectrum of the oxidized heme being affected by

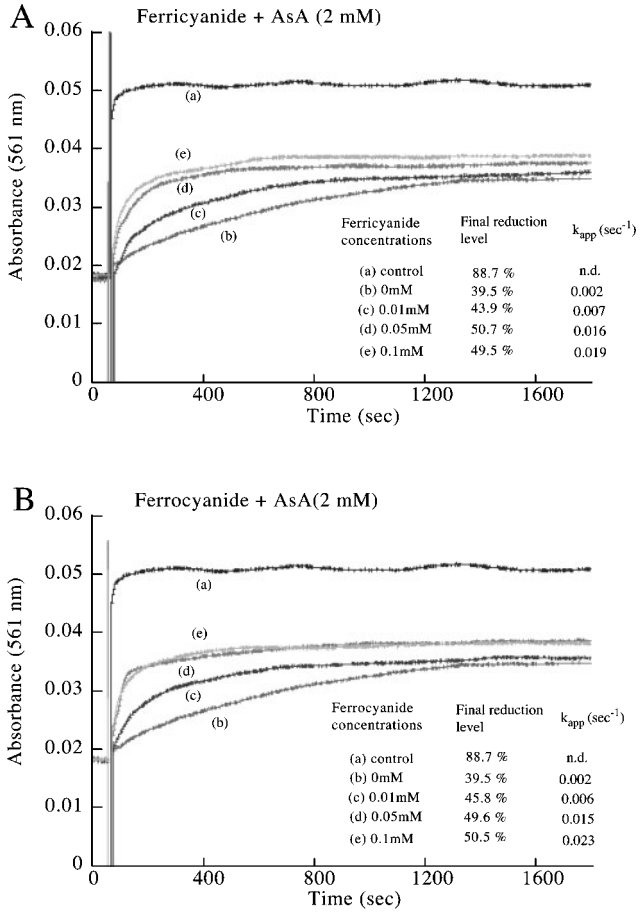

Fig. 5. **Effects of the addition of ferricyanide (A) and ferrocyanide (B) on the reduction of DEPC-treated cytochrome b_{561} with AsA.** Ferricyanide or ferrocyanide [final concentrations: (c), 0.01 mM; (d), 0.05 mM; and (e), 0.1 mM] was added to the oxidized form of DEPC-treated cytochrome b_{561} (1.5 μM) in 50 mM potassium-phosphate buffer (pH 6.0) containing 1.0% (w/v) octyl β-glucoside before the addition of AsA (final 2.0 mM). As a control, AsA (2.0 mM) alone was added to the oxidized form of DEPC-treated cytochrome b_{561} (b). For comparison, the reduction of the oxidized form of native cytochrome b_{561} upon the addition of AsA (2.0 mM) is also presented (a). Changes in the absorbance at 561 nm at 20°C were recorded with a UV-2400PC spectrophotometer. Although the absorbance changes in the presence of ferricyanide/ferrocyanide comprise more than two phases, only the first phases were analyzed based on pseudo first-order kinetics and their apparent rate constants (k_{app}) were calculated. The apparent rate constant (k_{app}) for the control sample determined by a stopped- flow method was 14.7 s^{-1} at pH 6.0 with AsA = 2.0 mM (*27*).

DEPC-treatment. However, the spectrum did not show any significant difference from the fully oxidized spectrum (spectra not shown). These results confirm that DEPC-treatment does not modify the chemical structure of the heme, but instead affects the redox level of the heme *b* center on the extravesicular side through the protein moiety.

We analyzed extensively the lower frequency region of the Raman spectra where the ligand-heme iron stretching modes are expected to appear. Indeed, the 272-cm^{-1} band of neutrophil cytochrome b_{558} in the oxidized form was assigned previously to a symmetric stretching frequency of the axial iron-imidazole (Fe^{3+}-N) bond (*44*),

although weak bands assignable to the ν_9 mode were observed at 276 and 263 cm^{-1} for the $[(Im)_2Fe^{3+}PP]^+$ and $(Im)_2Fe^{2+}PP$ model complexes, respectively (Table 1). It must be noted that the symmetric (ImH)-Fe-(ImH) stretch was assigned on the basis of its imidazole ^{15}N and a perdeuteration shift to a weak Soret-enhanced resonance Raman band at ~200 cm^{-1} for both $[(Im)_2Fe^{3+}PP]^+$ and $(Im)_2Fe^{2+}PP$ complexes (*42*), close to the corresponding py-Fe-py (py=pyridine) frequency 179 cm^{-1}, of $(py)_2Fe^{2+}MP$ (*49*). An L-Fe-L triatomic model in which L was given a point mass of the molecular weight of pyridine gave nearly the correct frequency. The shift upon deuteration of pyridine was also reproduced with this model (*49*). Therefore, if the 270-cm^{-1} band is indeed the axial-imidazole stretching band, it is to be expected that *N*-carbethoxylation of the imidazole ring would cause a significant down shift in its frequency (Im = 68.08, carbethoy group = 73). Since the imidazole group was jointed to protein backbone, the effective mass difference between the intact imidazole and *N*-carbethoxylated imidazole might not be very significant, but still large enough to be detected. The absence of the shift as shown in the present study suggests that the 270-cm^{-1} band is not an axial iron-imidazole (Fe^{3+}-N) stretching vibration and, therefore, we assigned it as the ν_9 mode.

Effects of Ferricyanide/Ferrocyanide on the Reduction of DEPC-Treated Cytochrome b_{561} with AsA—Treatment of oxidized cytochrome b_{561} with DEPC caused a significant decrease in the apparent reduction rate (k_{app}) and the final reduction level of cytochrome b_{561} when AsA (2 mM) was used as a reductant [Fig. 5A (b)], as previously described (*25*). The presence of ferricyanide (0.01–0.1 mM) before the addition of AsA (2 mM) restored significantly the apparent reduction rate (k_{app}) of the DEPC-treated cytochrome b_{561} [Fig. 5A (c, d, e)], although the time course of the absorbance change consisted of more than two phases. The restoration effect was also seen when ferricyanide was added after the addition of AsA (data not shown). The final reduction level also increased as the concentration of ferricyanide increased (0.01, 0.05, and 0.1 mM) [Fig. 5A (c, d, e)]. It was considered that ferrocyanide rather than ferricyanide is the effective species since ferricyanide might be converted almost completely to ferrocyanide (ferricyanide/ferrocyanide couple; $E_{m,7}$ = +425 mV) (*50*) in the presence of 2 mM AsA. As expected, similar restoring effects were observed when ferrocyanide (0.01, 0.05, and 0.1 mM) [Fig. 5B (c, d, e)] was used instead of ferricyanide. Although not so significant as ferricyanide/ferrocyanide, Fe^{3+}-EDTA also showed a restoring effect only on the final reduction level (data not shown). It must be noted that, although the restoration effects of ferricyanide/ferrocyanide were significant, the enhanced apparent reduction rate (k_{app}) was still much lower than that of the control sample [Fig. 5A (a)] and the final reduction level was at most 50% [Fig. 5A (c, d, e) and 5B (c, d, e)].

DISCUSSION

Absence of pH-Dependency in the Redox Potential of Two Heme b Centers—The Nernst plot for redox titration of purified cytochrome b_{561} showed a sigmoidal shape

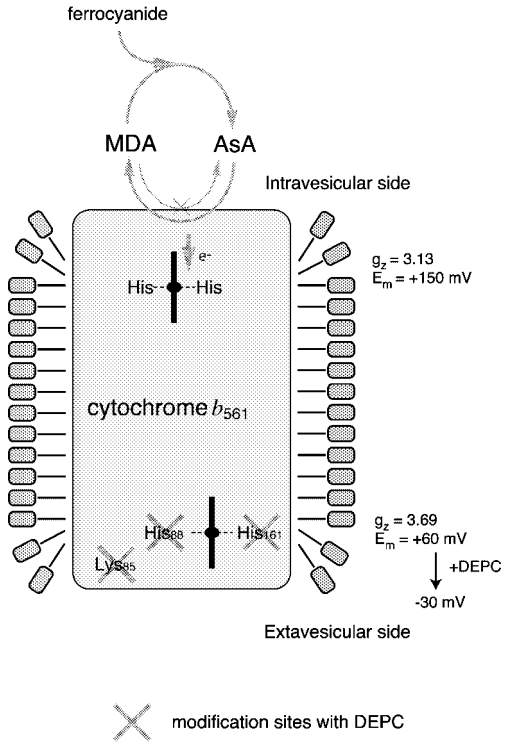

Fig. 6. **Schematic representation of the scavenging effect of ferrocyanide on the MDA radical produced by the univalent oxidation of AsA by DEPC-treated cytochrome b_{561}.** Three major DEPC-modification sites (Lys85, His88, and His161) are indicated. The heme *b* center on the extravesicular side (g_z = 3.69), therefore, does not participate in the redox reaction with AsA and the MDA radical; whereas the heme *b* center on the intravesicular side (g_z = 3.13) can accept electron equivalents from AsA to produce the MDA radical. The MDA radical can accept electron equivalents very quickly from the reduced heme *b* center on the intravesicular side, leading to the coexistence of the oxidized and reduced forms of heme *b*. The addition of ferrocyanide causes a quick reduction of the MDA radical to regenerate AsA and, thereby, eliminates the MDA radical from the system, leading to net increases in the apparent reduction rate (k_{app}) and final reduction level of heme *b* on the intravesicular side.

with the upper and lower asymptotic potentials estimated to be around +150 and +60 mV, respectively. This observation is very similar to previous reports (*26*, *39*), and is fully consistent with the notion of two heme *b* centers with different midpoint potentials on the intravesicular and extravesicular sides (*25*). It is very interesting to note that there was no appreciable pH-dependent change in the midpoint potential of either component of cytochrome b_{561}, although the measurements were done only in the acidic region (from pH 5.15 to 6.89). However, our previous pulse radiolysis study (*24*) showed that each of the electron transfer reactions with the MDA radical and AsA exhibited distinct and clear pH-dependency. Further, our recent stopped-flow study on the electron transfer from AsA to oxidized cytochrome b_{561} showed a strong pH-dependency (*27*). It is very probable that the observed pH-dependency in the fast reaction kinetics might reflect the presence of charged amino acid residue(s) responsible for the interaction with AsA and the MDA radical (see discussion in the next section). On the other hand, the

macroscopic redox level of the heme center might be controlled or modulated by many factors including the orientation of axial imidazole ligands (*51*, *52*), polarity of the heme microenvironment (*53*, *54*), and hydrogen bonding to the axial imidazole ligand (*55*), and, therefore, might not necessarily be dependent on the medium pH.

Effects of DEPC-Modification—The present study confirms our previous observation that the treatment of oxidized cytochrome b_{561} with DEPC causes a significant decrease in the lower asymptotic potential from +60 mV to –30 mV without affecting the higher asymptotic potential (Fig. 1) (*26*). As the cause of lowering of the redox potential, several possibilities may be considered. We showed previously that major DEPC-modification sites in the oxidized form include Lys85, His161, and either His88 or His92 (*25*), of which His88 and His161 have been postulated to be the heme axial ligands on the extravesicular side on the basis of the amino acid sequences of cytochrome b_{561} from various animals (*22*). Although our MALDI-TOF MS analyses could not distinguish between the two possible modification sites (His88 or His92), we believe that His88 is the more likely modification site since His92 should be located much deeper in the interior of the molecule. The *N*-carbethoxylation of the two His residues leads to a selective loss of electron accepting ability from AsA without affecting the electron donating ability to the MDA radical (Fig. 6) (*25*). Since the heme iron-imidazole coordination is intact after treatment with DEPC, the carbethoxylation should occur at the non-coordinating nitrogen atom of the imidazole group (usually Nδ) of His88 and His161, and this might be the main cause for the drastic lowering of the midpoint potential. DEPC-treatment in the oxidized state caused a conversion of the $g_z = 3.69$ species to a non-AsA-reducible form (but one fully reducible with sodium dithionite). This result suggests strongly that the $g_z = 3.69$ signal is derived from the heme *b* center on the extravesicular side of the cytochrome b_{561} molecule. Accordingly, the $g_z = 3.13$ signal is due to the other heme *b* center on the intravesicular side and is reducible with AsA as in the native form after DEPC-treatment. This conclusion is consistent with our previous assignment of the $g_z = 3.70$ species to have a lower midpoint potential than the $g_z = 3.14$ species, based on the EPR spectrum of the partially reduced form (*16*).

The drastic lowering of the midpoint potential of the heme *b* on the extravesicular side upon DEPC-modification might be explained by additional factor(s), such as a change in the polarity around the heme *b* or a subtle change in the conformation in the vicinity of the imidazole ring by *N*-carbethoxylation. The presence of AsA during the reaction with DEPC was found to suppress the *N*-carbethoxylation of the heme-coordinating histidyl residues (His88 and His161) significantly (*26*). Concomitantly, the downshift of the lower asymptotic potential was inhibited almost completely, although the fast reduction process was not fully restored (*26*, *27*). These results suggest that there is an AsA-binding site close to the heme *b* on the extravesicular side. This site might be formed by amino acid residues with positive charges interacting with a negatively charged AsA molecule. Further, a certain amino acid residue(s) at the site may facilitate the electron transfer from AsA to oxidized heme *b* by participating as a proton acceptor from AsA, as suggested by Njus and coworkers (*9*, *56*). There is a possibility that His88 or His161 plays such a dual role (*i.e.*, ligation to heme *b* and interaction with AsA).

Implications from the Resonance Raman Spectra—The presence of several Raman bands attributable to motions of heme vinyl substituent groups (Table 1) is consistent with the macrocycle being protoporphyrin IX. The resonance Raman data indicate further that both heme *b* centers of cytochrome b_{561} adopt six-coordinated low-spin states, both in the reduced and oxidized forms, in the sense that all major bands appearing in the model heme complex are also detectable at nearly identical frequencies in cytochrome b_{561} (Table 1). There was no indication suggesting a structural difference between the two heme *b* centers in the native cytochrome. In the higher frequency region, there was no difference between the DEPC-treated and native samples, in either the reduced or oxidized forms. DEPC-treatment in the oxidized form, however, caused the conversion of the heme *b* center at the extravesicular side to a non-reducible form with AsA. Resonance Raman and visible absorption data indeed confirmed that about two-thirds of the heme *b* center could not be reduced by 2 mM AsA (Fig. 4, A and B). One may suggest that only about one-third, instead of two-thirds, of heme *b* is not reduced by 2 mM AsA based on the comparison of Raman intensities of the ν_4 bands at 1,372 cm^{-1} and at 1,358 cm^{-1} in Fig. 4B (trace c). However, this can be explained as being due to the difference in intrinsic Raman intensities of the ν_4 band between the oxidized and reduced forms. The intensity of Raman scattering is determined by the polarizability tensor (*57*). Therefore, the Soret scattered intensity can be represented by a Franck-Condon mechanism and is approximated with functions of laser frequency, Soret band maximum, Soret band width, and the molar extinction coefficient at the excitation frequency (*58*). It must be noted that the addition of dithionite to the DEPC-treated sample caused a complete conversion to the fully-reduced form (Fig. 4A), and the Raman spectrum was indistinguishable from that of the native sample. We also analyzed the lower frequency region of the Raman spectra, expecting the ligand-heme iron stretching modes to be identified. Neither the 270-cm^{-1} band, a possible candidate for the symmetric (ImH)-Fe-(ImH) stretch, nor any other band in this region showed any considerable shift upon the *N*-carbethoxylation of the imidazole ring, suggesting that the 270-cm^{-1} band is not an axial iron-imidazole (Fe^{3+}-N) stretching vibration and, therefore, we assigned it as the ν_9 mode.

Effects of Ferricyanide/Ferrocyanide on the Reduction of the DEPC-Treated Cytochrome b_{561} with AsA—One may be puzzled that the final reduction level of the DEPC-treated cytochrome b_{561} with AsA is around 35–40% (in the absence of ferricyanide/ferrocyanide). Since DEPC-treatment should affect the low-potential heme *b* center on the extravesicular side alone, the final reduction level should reach as high as the 50% level, which corresponds to the full reduction of the high-potential heme *b* center on the intravesicular side. This apparent discrepancy can be explained as follows. Upon mixing AsA with the oxidized form of DEPC-treated cytochrome b_{561} in the detergent-solubilized state, the MDA radical might be produced by the univalent oxidation of AsA by

direct electron transfer to the heme *b* center on the intravesicular side (Fig. 6). It must be noted that the reaction is very slow, since its direction is a reversal of the physiological electron transfer. Simultaneously, the oxidation of the reduced heme *b* on the intravesicular side by the MDA radical just produced should occur, since this heme center has a significant activity towards the MDA radical (*24*). Therefore, the final reduction level of 35–40% for the DEPC-treated cytochrome b_{561} with AsA (*25*) is a reflection of the balance of two opposing reactions (*i.e.*, reduction by AsA and oxidation by the MDA radical at the heme *b* center on the intravesicular side).

Considering the situation of the DEPC-treated cytochrome b_{561} as described above, we rationalized the restoration effects of ferricyanide/ferrocyanide as follows. The apparent reduction rate (k_{app}) and the final reduction level of the DEPC-treated cytochrome b_{561} with AsA as a reductant are increased significantly upon the addition of ferricyanide/ferrocyanide, but never reach the levels observed for the control sample (Fig. 5, A and B). Although ferricyanide is known to oxidize the MDA radical very efficiently (*50*), ferrocyanide rather than ferricyanide might be the active species for the restoration effects. However, since the addition of ferrocyanide alone has no effect on the oxidized form of cytochrome b_{561} irrespective of the DEPC-treatment (results not shown), direct electron transfer from ferrocyanide to the oxidized heme *b* of the DEPC-treated cytochrome b_{561} can be ruled out as the cause.

The most likely explanation for the restoration effect of ferrocyanide is that it acts as a scavenger of the MDA radical. Ferrocyanide can donate an electron equivalent to the MDA radical very quickly to regenerate AsA and, thereby, eliminates the MDA radical from the system (Fig. 6). This will cause a net increase in the apparent reduction rate (k_{app}) of heme *b* on the intravesicular side. Simultaneously, an increase in the final reduction level of heme *b* on the intravesicular side due to the net decrease in the redox potential of the AsA/MDA radical couple might occur. This scheme is consistent with the notion that the heme *b* center on the extravesicular side is not involved in the restoration effects and that the final reduction level does not exceed 50%.

The restoration effect of Fe^{3+}-EDTA may be explained by a similar mechanism. However, since the midpoint potential of the Fe^{3+}-EDTA/Fe^{2+}-EDTA couple ($E_{m,7}$ = +117 mV) (*59*) is much lower than that of the ferricyanide/ferrocyanide couple, it is not clear whether Fe^{2+}-EDTA is actually involved in scavenging MDA radicals or not. Indeed, it has been reported that Fe^{3+}-EDTA itself is an efficient electron acceptor from the MDA radical (*60*). In either case, Fe^{3+}-EDTA/Fe^{2+}-EDTA might eliminate the MDA radical from the system by converting it to either dehydroascorbate or AsA and, thereby, restore the final reduction level of heme *b* on the intravesicular side.

Comments on the Presence of a Third Heme b Center—Kamensky *et al*. recently proposed that cytochrome b_{561} in chromaffin vesicle membranes might actually contain three heme *b* centers (*30*). In their model, cytochrome b_{561} forms a dimer with one high-potential heme per monomer and one low-potential heme per dimer (*30*). Therefore, the low-potential heme might be shared by two subunits as has been observed for photosynthetic cytochrome b_{559} (*61*), so vastly different from our present model. However, several pieces of evidence suggest that our model is more likely. First, our recent heme content analysis based on a pyridine hemochrome method and protein content determination with bovine serum albumin as a standard showed a value close to 2.0 hemes *b* per monomer rather than 1.5 (Takeuchi *et al*., unpublished). Second, the low-potential heme *b* center is actually much more resistant to denaturation by alkaline treatment than the other high-potential heme *b* center (*22*, *24*). This fact seems inconsistent with the view that the low-potential heme is located between two subunits and, therefore, might be more labile than the other heme center with a higher potential. Third, our present results in the AsA-reducing assay on DEPC-treated cytochrome b_{561} is more consistent with the view that DEPC-treatment causes 50% (not 33%) of the total heme center of cytochrome b_{561} to be converted to a non-reducible form with AsA. (If the Kamensky model is correct, the final reduction level with AsA should reach 66% in the presence of ferricyanide/ferrocyanide.) It must be noted, however, that our present data do not exclude the possibility that cytochrome b_{561} forms a dimer in chromaffin vesicle membranes.

In conclusion, the present redox titration, EPR, and resonance Raman data establish that both of the two heme *b* centers (the g_z = 3.69 and the g_z = 3.13 species) adopt six-coordinated low-spin states, in both the reduced and oxidized forms, but have different midpoint potentials. The g_z = 3.69 heme *b* center, which is likely to play a role in accepting an electron equivalent from AsA on the extravesicular side, can be converted to a non-reducible form with AsA upon DEPC-treatment due to a significant decrease in its midpoint potential. We found further that ferrocyanide scavenges the MDA radical produced by the univalent oxidation of AsA by DEPC-treated cytochrome b_{561} and, thereby, increases both the reduction rate and the final reduction level of the heme *b* center on the intravesicular side. These results further clarify the role of this heme center as the electron donor to the MDA radical.

This study was supported by Grants-in-Aid for Scientific Research on Priority Areas (Comprehensive Promotion of Study of Brain; 12050236 to M.T.) and (C) (12680659 and 14580676 to M.T.) from the Japanese Ministry of Education, Science, Sports and Culture. We thank to Drs. Takeshi Tomita and Teizo Kitagawa of IMS, Okazaki, Japan, for assistance with the preliminary measurements of the resonance Raman spectra of the partially purified cytochrome b_{561}.

REFERENCES

1. Rice, M.E. (2000) Ascorbate regulation and its neuroprotective role in the brain. *Trends Neurosci.* **23**, 209–216
2. Tsukaguchi, H., Tokui, T., Mackenzie, B., Berger, U.V., Chen, X.-Z., Wang, Y., Brubaker, R.F., and Hediger, M.A. (1999) A family of mammalian Na^+-dependent L-ascorbic acid transporters. *Nature* **399**, 70–75
3. Eipper, B.A., Mains, R.E., and Glembotski, C.C. (1983) Identification in pituitary tissue of a peptide α-amidation activity that acts on glycine-extended peptides and requires molecular oxygen, copper, and ascorbic acid. *Proc. Natl Acad. Sci. USA* **80**, 5144–5148
4. Kent, U.M. and Fleming, P.J. (1987) Purified cytochrome b_{561} catalyzes transmembrane electron transfer for dopamine β-

hydroxylase and peptidyl glycine α-amidating monooxygenase activities in reconstituted systems. *J. Biol. Chem.* **262**, 8174–8178
5. Dhariwal, K.R., Black, C.D.V., and Lavine, M. (1991) Semidehydroascorbic acid as an intermediate in norepinephrine biosynthesis in chromaffin granules. *J. Biol. Chem.* **266**, 12908–12914
6. Njus, D., Knoth, J., Cook, C., and Kelley, P.M. (1983) Electron transfer across the chromaffin granule membrane. *J. Biol. Chem.* **258**, 27–30
7. Njus, D., Kelley, P.M., and Harnadek, G.J. (1986) Bioenergetics of secretory vesicles. *Biochim. Biophys. Acta* **853**, 237–265
8. Wakefield, L.M., Cass, A.E.G., and Radda, G.K. (1986) Functional coupling between enzymes of the chromaffin granule membrane. *J. Biol. Chem.* **261**, 9739–9745
9. Njus, D. and Kelley, P.M. (1993) The secretory-vesicle ascorbate-regenerating system: a chain of concerted H^+/e^- transfer reactions. *Biochim. Biophys. Acta* **1144**, 235–248
10. Duong, L.T., Fleming, P.J., and Russell, J.T. (1984) An identical cytochrome b_{561} is present in bovine adrenal chromaffin vesicles and posterior pituitary neurosecretory vesicles. *J. Biol. Chem.* **259**, 4885–4889
11. Pruss, R.M. and Shepard, E.A. (1987) Cytochrome b_{561} can be detected in many neuroendocrine tissues using a specific monoclonal antibody. *Neuroscience* **22**, 149–157
12. Asada, A., Kusakawa, T., Orii, H., Agata, K., Watanabe, K., and Tsubaki, M. (2002) Planarian cytochrome b_{561}: Conservation of a six-transmembrane structure and localization along the central and peripheral nervous system. *J. Biochem.* **131**, 175–182
13. Silsand, T. and Flatmark, T. (1974) Purification of cytochrome *b*-561 An integral heme protein of the adrenal chromaffin granule membrane. *Biochim. Biophys. Acta* **359**, 257–266
14. Duong, L.T. and Fleming, P.J. (1982) Isolation and properties of cytochrome b_{561} from bovine adrenal chromaffin granules. *J. Biol. Chem.* **257**, 8561–8564
15. Pruss, R.M. (1987) Monoclonal antibodies to chromaffin cells can distingush proteins specific to or specifically excluded from chromaffin granules. *Neuroscience* **22**, 141–147
16. Tsubaki, M., Nakayama, M., Okuyama, E., Ichikawa, Y., and Hori, H. (1997) Existence of two heme B centers in cytochrome b_{561} from bovine adrenal chromaffin vesicles as revealed by a new purification procedure and EPR spectroscopy. *J. Biol. Chem.* **272**, 23206–23210
17. Burbaev, D.S., Moroz, I.A., Kamensky, Y.A., and Konstantinov, A.A. (1991) Several forms of chromaffin granule cytochrome *b*-561 revealed by EPR spectroscopy. *FEBS Lett.* **283**, 97–99
18. Perin, M.S., Fried, V.A., Slaughter, C.A., and Südhof, T.C. (1988) The structure of cytochrome b_{561}, a secretory vesicle-specific electron transport protein. *EMBO J.* **7**, 2697–2703
19. Srivastava, M., Gibson, K.R., Pollard, H.B., and Fleming, P.J. (1994) Human cytochrome b_{561}. A revised hypothesis for conformation in membranes which reconciles sequence and functional information. *Biochem. J.* **303**, 915–921
20. Srivastava, M. (1996) *Xenopus* cytochrome b_{561}: Molecular confirmation of a general five transmembrane structure and developmental regulation at the gastrula stage. *DNA Cell Biol.* **15**, 1075–1080
21. Srivastava, M., Pollard, H.B., and Fleming, P.J. (1998) Mouse cytochrome b561: cDNA cloning and expression in rat brain, mouse embryos, and human glioma cell lines. *DNA Cell Biol.* **17**, 771–777
22. Okuyama, E., Yamamoto, R., Ichikawa, Y., and Tsubaki, M. (1998) Structural basis for the electron transfer across the chromaffin vesicle membranes catalyzed by cytochrome b_{561}: Analyses of cDNA nucleotide sequences and visible absorption spectra. *Biochim. Biophys. Acta* **1383**, 269–278
23. Degli Esposti, M., Kamensky, Y.A., Arutjunjan, A.M., and Konstantinov, A.A. (1989) A model for the molecular organization of cytochrome b-561 in chromaffin granule membranes. *FEBS Lett.* **254**, 74–78
24. Kobayashi, K., Tsubaki, M., and Tagawa, S. (1998) Distinct roles of two heme centers for transmembrane electron transfer in cytochrome b_{561} from bovine adrenal chromaffin vesicles as revealed by pulse radiolysis. *J. Biol. Chem.* **273**, 16038–16042
25. Tsubaki, M., Kobayashi, K., Ichise, T., Takeuchi, F., and Tagawa, S. (2000) Diethylpyrocarbonate-modification abolishes fast electron accepting ability of cytochrome b_{561} from ascorbate but does not influence on electron donation to monodehydroascorbate radical: Distinct roles of two heme centers for electron transfer across the chromaffin vesicle membranes. *Biochemistry* **39**, 3276–3284
26. Takeuchi, F., Kobayashi, K., Tagawa, S., and Tsubaki, M. (2001) Ascorbate inhibits the carbethoxylation of two histidyl and one tyrosyl residues indispensable for the transmembrane electron transfer reaction of cytochrome b_{561}. *Biochemistry* **40**, 4067–4076
27. Takigami, T., Takeuchi, F., Nakagawa, M., Hase, T., and Tsubaki, M. (2003) Stopped-flow analyses on the reaction of ascorbate with cytochrome b_{561} purified from bovine chromaffin vesicle membranes. *Biochemistry* **42**, 8110–8118
28. Flatmark, T. and Terland, O. (1971) Cytochrome b_{561} of the bovine adrenal chromaffin granules. A high potential b-type cytochrome. *Biochim. Biophys. Acta* **253**, 487–491
29. Kamensky, Y.A. and Palmer, G. (2001) Chromaffin granule membranes contain at least three heme centers: direct evidence from EPR and absorption spectroscopy. *FEBS Lett.* **491**, 119–122
30. Kamensky, Y.A., Kulmacz, R.J., and Palmer, G. (2002) Composition of the heme centers in chromaffin granule cytochrome b_{561}. *Ann. N. Y. Acad. Sci.* **971**, 450–453
31. Wanduragala, S., Wimalasena, D.S., Haines, D.C., Kahol, P.K., and Wimalasena, K. (2003) pH-Induced alteration and oxidative destruction of heme in purified chromaffin granule cytochrome b_{561}: Implications for the oxidative stress in catecholaminergic neurons. *Biochemistry* **42**, 3617–3626
32. Mckie, A.T., Barrow, D., Latunde-Dada, G.O., Rolfs, A., Sager, G., Mudaly, E., Mudaly, M., Richardson, C., Barlow, D., Bomford, A., Peters, T.J., Raja, K.B., Shirali, S., Hediger, M.A., Farzaneh, F., and Simpson, R.J. (2001) An iron-regulated ferric reductase associated with the absorption of dietary iron. *Science* **291**, 1755–1759
33. Mckie, A.T., Latunde-Dada, G.O., Miret, S., McGregor, J.A., Anderson, G.J., Vulpe, C.D., Wriggleworth, J.M., and Simpson, R.J. (2002) Molecular evidence for the role of a ferric reductase in iron transport. *Biochem. Soc. Trans* **30**, 722–724
34. Escriou, V., Laporte, F., Garin, J., Brandolin, G., and Vignais, P.V. (1994) Purification and physical properties of a novel type of cytochrome *b* from rabbit peritoneal neutrophils. *J. Biol. Chem.* **269**, 14007–14014
35. Horemans, N., Foyer, C.H., and Asard, H. (2000) Transport and action of ascorbate at the plant plasma membrane. *Trends Plant Sci.* **5**, 263–267
36. Trost, P., Bérczi, A., Sparla, F., Sponza, G., Marzadori, B., Asard, H., and Pupillo, P. (2000) Purification of cytochrome b_{561} from bean hypocotyls plasma membrane. Evidence for the presence of two heme centers. *Biochim. Biophys. Acta* **1468**, 1–5
37. Ponting, C.P. (2001) Domain homologues of dopamine β-hydroxylase and ferric reductase: roles for iron metabolism in neurodegenerative disorders? *Hum. Mol. Genet.* **10**, 1853–1858
38. Dutton, P.L. (1978) Redox potentiometry: Determination of midpoint potentials of oxidation-reduction components of biological electron-transfer systems. *Methods Enzymol.* **54**, 411–435
39. Apps, D.K., Boisclair, M.D., Gavine, F.S., and Pettigrew, G.W. (1984) Unusual redox behaviour of cytochrome *b*-561 from bovine chromaffin granule membranes. *Biochim. Biophys. Acta* **764**, 8–16
40. Kitagawa, T. and Ozaki, Y. (1987) Infrared and Raman spectra of metalloporphyrins. *StructureBonding* **64**, 71–114
41. Choi, S., Spiro, T.G., Langry, K.C., Smith, K.M., Budd, D.L., and La Mar, G.N. (1982) Structural correlations and vinyl

influences in resonance Raman spectra of protoheme complexes and proteins. *J. Amer. Chem. Soc.* **104**, 4345–4351
42. Choi, S. and Spiro, T.G. (1983) Out-of-plane deformation modes in the resonance Raman spectra of metalloporphyrins and heme proteins. *J. Amer. Chem. Soc.* **105**, 3683–3692
43. Flatmark, T., Terland, O., and Helle, K.B. (1971) Electron carriers of the bovine adrenal chromaffin granules. *Biochim. Biophys. Acta* **226**, 9–19
44. Hurst, J.K., Loehr, T.M., Curnutte, J.T., and Rosen, H. (1991) Resonance Raman and electron paramagnetic resonance structural investigations of neutrophil cytochrome b_{558}. *J. Biol. Chem.* **266**, 1627–1634
45. Fujii, H., Finnegan, M.G., Miki, T., Crouse, B.R., Kakinuma, K., and Johnson, M.K. (1995) Spectroscopic identification of the heme axial ligation of cytochrome b_{558} in the NADPH oxidase of porcine neutrophils. *FEBS Lett.* **377**, 345–348
46. Babcock, G.T., Widger, W.R., Cramer, W.A., Oertling, W.A., and Metz, J.G. (1985) Axial ligands of chloroplast cytochrome *b*-559: Identification and requirement for a heme-cross-linked polypeptide structure. *Biochemistry* **24**, 3638–3645
47. Kitagawa, T., Kyogoku, Y., Iizuka, T., Ikeda-Saito, M., and Yamanaka, T. (1975) Resonance Raman scattering from hemoproteins effeect of ligands upon the Raman spectra of various C-type cytochromes. *J. Biochem.* **78**, 719–728
48. Kitagawa, T., Kyogoku, Y., Iizuka, T., and Saito, M.I. (1976) Nature of the iron-ligand bond in ferrous low spin hemoproteins studied by resonance Raman scattering. *J. Amer. Chem. Soc.* **98**, 5169–5173
49. Wright, P.G., Stein, P., Burke, J.M., and Spiro, T.G. (1979) Resonance Raman spectra, excitation profiles and excited (iron–pyridine charge transfer) state geometry of bispyridine iron (II) heme. *J. Amer. Chem. Soc.* **101**, 3531–3535
50. Iyanagi, T., Yamazaki, I., and Anan, K.F. (1985) One-electron oxidation-reduction properties of ascorbic acid. *Biochim. Biophys. Acta* **806**, 255–261
51. Safo, M.K., Gupta, G.P., Walker, F.A., and Scheidt, W.R. (1991) Models of the cytochromes *b*. Control of axial ligand orientation with a "hindered" porphyrin system. *J. Amer. Chem. Soc.* **113**, 5497–5510
52. Sarma, S., DiGate, R.J., Goodin, D.B., Miller, C.J., and Guiles, R.D. (1997) Effect of axial ligand plane reorientation on electronic and electrochemical properties observed in the A67V mutant of rat cytochrome b_5. *Biochemistry* **36**, 5658–5668
53. Langen, R., Brayer, G.D., Berghuis, A.M., McLendon, G., Sherman, F., and Warshel, A. (1992) Effects of the Asn52→Ile mutation on the redox potential of yeast cytochrome *c*. Theory and experiment. *J. Mol. Biol.* **224**, 589–600
54. Xue, L.-L., Wang, Y.-H., Xie, Y., Yao, P., Wang, W.-H., Qian, W., and Huang, Z.-X. (1999) Effect of mutation at valine 61 on the three-dimensional structure, stability, and redox potential of cytochrome b_5. *Biochemistry* **38**, 11961–11972
55. Goodin, D.B. and McRee, D.E. (1993) The Asp-His-Fe triad of cytochrome *c* peroxidase controls the reduction potential, electronic structure, and coupling of the tryptophan free radical to the heme. *Biochemistry* **32**, 3313–3324
56. Jalukar, V., Kelley, P.M., and Njus, D. (1991) Reaction of ascorbic acid with cytochrome b_{561} Concerted electron and proton transfer. *J. Biol. Chem.* **266**, 6878–6882
57. Babcock, G.T., Callahan, P.M., Ondrias, M.R., and Salmeen, I. (1981) Coordination geometries and vibrational properties of cytochrome *a* and a_3 in cytochrome oxidase from Soret excitation Raman spectroscopy. *Biochemistry* **20**, 959–966
58. Ondrias, M.R. and Babcock, G.T. (1980) Resonance enhancement of the vibrations of cytochrome a_3 and its conformation in oxidized cytochrome oxidase. *Biochem. Biophys. Res. Commun.* **93**, 29–35
59. Ilan, Y.A. and Czapski, G. (1977) The reaction of superoxide radical with iron complexes of EDTA studied by pulse radiolysis. *Biochim. Biophys. Acta* **498**, 386–394
60. Kobayashi, K., Harada, Y., and Hayashi, K. (1991) Kinetic behavior of the monodehydroascorbate radical studied by pulse radiolysis. *Biochemistry* **30**, 8310–8315
61. McNamara, V.P., Sutterwala, F.S., Pakrasi, H., and Whitmarsh, J. (1997) Structural model of cytochrome b_{559} in photosystem II based on a mutant with genetically fused subunits. *Proc. Natl Acad. Sci. USA* **94**, 14173–14178
62. Abe, M., Kitagawa, T., and Kyogoku, Y. (1978) Resonance Raman spectra of octaethylporphyrinato-Ni(II) and meso-deuterated and ^{15}N substituted derivatives. II. A normal coordinate analysis. *J. Chem. Phys.* **69**, 4526–4534